Mem. S.A.It. Vol. 84, 363
© SAIt 2013
Memorie della

Spatial distribution of the magnetic helicity flux measured with SDO/HMI in active regions hosting flares and CMEs

P. Romano[1] and F. Zuccarello[2]

[1] Istituto Nazionale di Astrofisica – Osservatorio Astrofisico di Catania, Via S. Sofia 78, 95123, Catania, Italy, e-mail: `paolo.romano@oact.inaf.it`
[2] Universitá di Catania, Dipartmento di Fisica e Astronomia, Via S. Sofia 78, 95123, Catania, Italy

Abstract. The study of the accumulation of magnetic helicity via emergence of new magnetic flux and/or shearing photospheric motions is considered an important tool for understanding the processes that lead to eruptive phenomena. In a previous work we measured the amount of magnetic helicity injected into the corona through the photosphere in a sample of active regions (ARs) by inferring the apparent motion of photospheric footpoints of magnetic field lines from a time series of MDI full-disk line-of-sight magnetograms (Romano & Zuccarello 2011). The temporal variation of the maps of magnetic helicity flux was analysed by measuring the fragmentation of the patches characterized by different flux of magnetic helicity. The more fragmented were the maps of the magnetic helicity flux, the higher was the flare and coronal mass ejection (CME) frequency. In order to further investigate the correlation between the number of these patches and the flare and the CME occurrence, another sample of ARs observed with a higher spatial resolution by SDO/HMI has been analyzed. The new results indicate that not only the accumulation of magnetic helicity in the corona, but also its positive and negative fragmentation and distribution should be taken into account to provide a more confident indication of AR complexity and flare/CME productivity.

Key words. Sun: activity – Sun: flares – Sun: coronal mass ejections (CMEs) – Sun: magnetic topology

1. Introduction

Coronal mass ejections (CMEs) are complex phenomena that can involve all the solar atmospheric layers, releasing up to 10^{32} erg of energy and ejecting more than 10^{16} g of solar plasma into interplanetary space. Often these events are spatially and timely correlated to solar flares. Recent advances in the understanding of the theory of such events have indicated that a catastrophic loss of mechanical equilibrium in a complex coronal magnetic configuration could be the trigger for major eruptions (Priest et al. 2000). Moreover, the loss of equilibrium drives magnetic reconnection in the magnetic field, which is stretched out by the eruption itself (Lin et al. 2003). The more complex is the magnetic field configuration,

Send offprint requests to: P. Romano

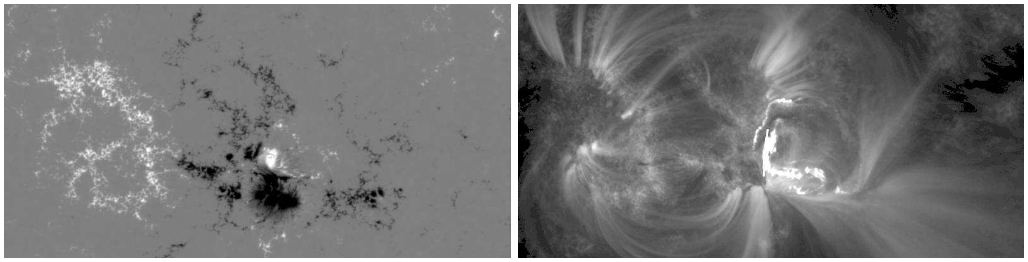

(a) (b)

Fig. 1. (a) Line of sight magnetogram of the AR NOAA 11238 acquired by HMI/SDO on Sept. 6 at 22:24 UT. (b) 171 Å image taken by AIA/SDO on Sept. 6 at 22:17 UT. The field of view is of about 400 × 200 arcsec^2 (290 × 145 Mm^2). North is at the top, west is on the right.

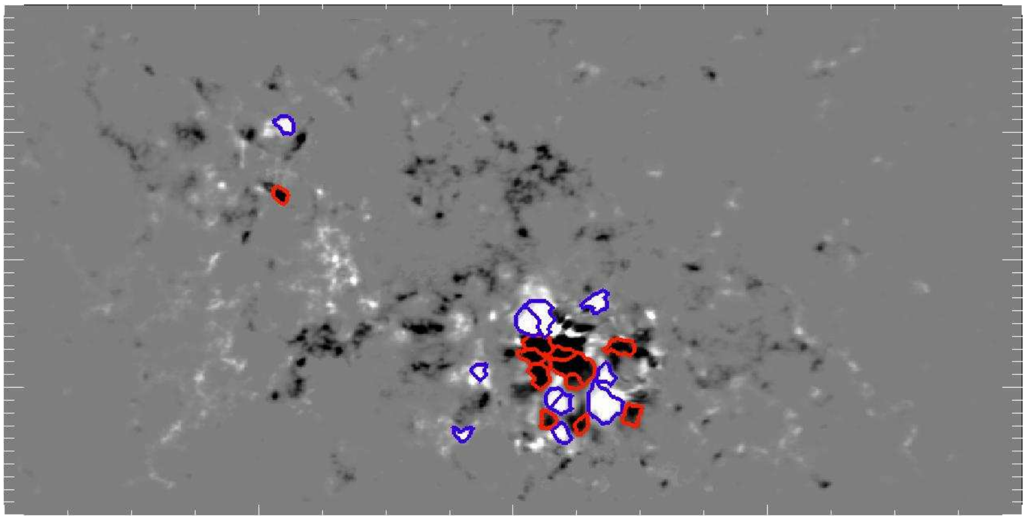

Fig. 2. Helicity flux density map computed with the method of Pariat et al. (2005) using the magnetograms taken on Sept. 8, at 14:24 UT and at 16:00 UT. Black and white correspond to negative and positive helicity flux density, respectively. The saturation levels are $\pm$ 1.5 × 10^{18} Mx^2 cm^{-2} s^{-1}; red and blue contours indicate elements of negative and positive helicity flux determined by the YAFTA feature-tracking algorithm, respectively. The field of view and the orientation are the same as in Fig. 1.

the higher is the probability of a catastrophic loss of equilibrium.

A useful topological quantity which measures the complexity of the magnetic field configuration is the magnetic helicity, H. It quantifies the twist, the writhe and the shear of a magnetic field system and, therefore, may be a key quantity to understand the onset mechanism of flares and CMEs. The direct computation of magnetic helicity in a solar active region (AR) requires knowledge of the magnetic field connectivity in the entire volume under study, but since magnetic field measurements are mainly done at the photospheric level, the most common way to estimate magnetic helicity is through the computation of the magnetic helicity flux from the convection zone (dH/dt).

However, current methods used for the determination of the helicity flux exhibit spurious signals, which affect the spatial distribution of the helicity flux density and do not provide the true helicity flux density distribution.

In fact, fake polarities appear when two different magnetic polarities are moving one with respect to the other and when a new flux tube is emerging. In this regard, Pariat et al. (2005) proposed a new method which is able to partially remove these fake polarities and represents a better proxy to the helicity flux density calculation.

Romano & Zuccarello (2011) applied this method to a sample of ARs observed by MDI/SOHO and previously studied by Nindos et al. (2003). They analysed the temporal variation of the maps of magnetic helicity flux by measuring the fragmentation of the patches, determined grouping unipolar, contiguous pixels with a helicity flux density greater than $5{\cdot}10^{17}$ Mx^2 cm^{-2} s^{-1} in absolute value. In particular, they studied the temporal correlation between the number of these patches and the flare and CME occurrence, finding that the fragmentation of the patches provided a useful indication of the evolution of AR complexity. The more fragmented the maps of the magnetic helicity flux were, the higher was the flare and CME frequency. Moreover, most of the events occurred for low values of the difference of the number of patches with opposite signs of magnetic helicity flux, suggesting that the coexistence of systems characterized by opposite sign of magnetic helicity flux may be responsible for many observed events.

The aim of this Paper is to apply the same analysis of Romano & Zuccarello (2011) to line-of-sight magnetograms acquired by HMI/SDO (Schou et al. 2012) at 6173 Å, in order to verify the temporal correlation between the fragmentation of the helicity flux maps and the flare and the CME occurrence. In fact, the better spatial resolution of HMI/SDO (1.02 arcsec) with respect to MDI/SOHO (3.96 arcsec) represents a new chance to investigate in more detail the distribution of the helicity flux density. For this reason we selected as target the AR NOAA 11238, where 4 flares and associated CMEs occurred during the selected time interval. This target and the corresponding HMI/SDO data are described in Section 2, while the results and the conclusions are reported in Sections 3 and 4, respectively.

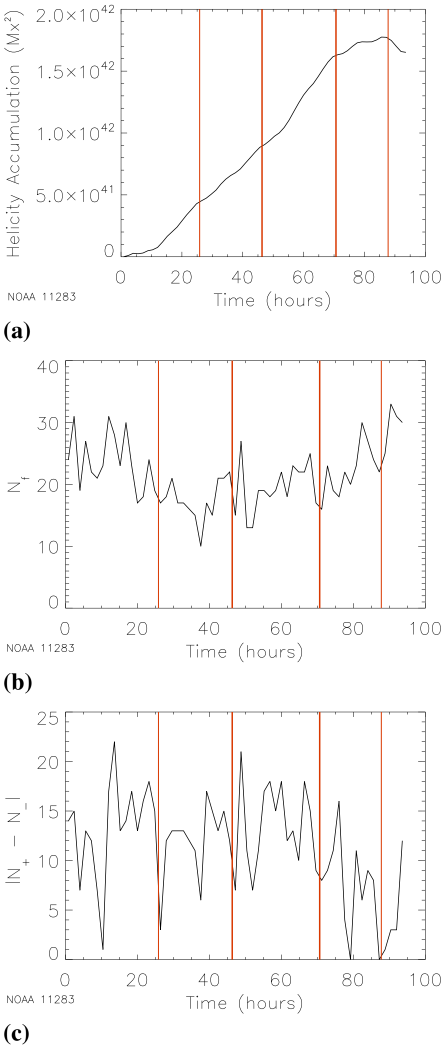

Fig. 3. (a) Accumulation of the magnetic helicity vs time. (b) Number of patches determined by the YAFTA algorithm vs time. (c) Absolute value of the difference between the numbers of positive and negative patches vs time. t=0 corresponds to 00:00 UT on Sept. 5, 2011. The red vertical lines indicate the flare/CME occurence. The thickness of the vertical lines is equal to 1 and 2 for flares of GOES M and X classes, respectively.

2. Observations and analysis

We analyzed the full-disk line-of-sight magnetograms acquired by HMI/SDO at 6173 Å from Sept. 5, 2011 at 00:00 UT to Sept. 8, 2011 at 22:24 UT with a spatial resolution of 1.02 arcsec in order to study the AR NOAA 11283. The GOES M and X-class flares occurred in the AR during this time interval are reported in Table 1. All these events occurred at the same time of CMEs observed by LASCO/SOHO and reported in the LASCO catalogue (http://cdaw.gsfc.nasa.gov/CME_list/). The photospheric configuration of the AR at the beginning of the selected time interval was characterized by a preceding main sunspot of negative polarity and by following pores of positive polarity. The sequence of magnetograms shows the emrgence of a new positive magnetic feature near the main negative polarity during the observation interval. This new feature moves eastwards while the negative one moves in the opposite direction. Probably, the shear of the magnetic field lines connecting the two polarities played an important role in the storage of magnetic energy released during the events occurred till the AR reached the solar limb. In fact, AIA/SDO images of the corona taken during the events show brightenings in the western part of the AR, i.e. corresponding to the emergence area, as reported in Fig. 1(b) for the second event reported in Table 1.

In order to compare the results obtained in this work with those obtained in Romano & Zuccarello (2011), we mantained the same temporal resolution using magnetograms taken with a time cadence of 96 min. We corrected all the magnetograms for the angle between the magnetic field direction and the observer's line-of-sight. All the subfields were aligned by applying a standard differential rotation rate (Howard et al. 1990) with a sampling of 0.5 arcsec. As in Romano & Zuccarello (2011), we determined the mean magnetogram corresponding to the average between two consecutive magnetograms and we measured the horizontal velocity fields by means of the Differential Affine Velocity Estimator (DAVE) method (Schuck 2005) using a full width at half maximum of the apodization window of 19.80 arcsec. Then we used these measurements to compute the magnetic helicity flux with the method of Pariat et al. (2005).

Finally, we applied the labelling algorithm YAFTA (a single-pass "flux-ranked uphill gradient" algorithm described in Welsch & Longcope (2003) on the helicity maps to group contiguous pixels into features (patches) that we defined to be convex groupings of 100 or more unipolar, contiguous pixels with a helicity flux density greater than $5{\cdot}10^{17}$ Mx^2 cm^{-2} s^{-1} in absolute value. An example of the patches determined by the algorithm is shown in Fig. 2. For each map we computed the total number of the identified patches, N_f, and the absolute value of the difference between the number of patches of the two signs, $|N_+ - N_-|$.

3. Results

In Fig. 3(a) we report the magnetic helicity accumulation deduced using the Pariat et al. (2005) method. We indicate in the same plot by vertical lines the time when the main flares and the associated CMEs occurred. We note that the AR was characterized by a prevalent positive flux of magnetic helicity. The magnetic helicity accumulated in the AR is 1.8×10^{42} Mx^2 in about 4 days. Only at the end of the selected time interval the helicity accumulation curve changes its slope. This effect could be ascribed to the limits of the correction for the angle between the magnetic field direction and the observer's line-of-sight as well as to the application of the standard differential rotation rate, due to the longitude of the AR (between 30 W and 43 W on Sept. 8). However, we note that no significant variation of the helicity accumulation trend is found when flares/CMEs occurred.

The variation of the number of patches determined by the YAFTA algorithm on the helicity flux density maps as a function of time is reported in Fig. 3 (b). As we can see from the comparison between the ARs analysed in (Romano & Zuccarello 2011) and the AR NOAA 11238 (see Table 2), despite the better spatial resolution of the HMI/SDO magnetograms with respect to those acquired by MDI, the AR NOAA 11283 appears less fragmented than the others: at maximum the algorithm YAFTA identified 33 patches. Moreover, the standard deviation of N_f is 5.08 indicating

Table 1. List of the flares occurred in AR NOAA 11283 during the observation interval, reported by the Space Environment Center. (http://www.swpc.noaa.gov/)

Date	Start (UT)	Peak (UT)	End (UT)	GOES class
6-9-2011	01:35	01:50	02:05	M5.3
6-9-2011	22:12	22:20	22:24	X2.1
7-9-2011	22:32	22:38	22:44	X1.8
8-9-2011	15:32	15:46	15:52	M6.7

Table 2. Comparison of maximum, minimum and standard deviation of N_f and $|N_+ - N_-|$ for the ARs analyzed in Romano & Zuccarello (2011) and for AR NOAA 11238 considered in this Paper.

NOAA	Max_{N_f}	Min_{N_f}	σ_{N_f}	$\mathrm{Max}_{\lvert N_+-N_-\rvert}$	$\mathrm{Min}_{\lvert N_+-N_-\rvert}$	$\sigma_{\lvert N_+-N_-\rvert}$
8210	62	21	9.30	34	1	7.77
8375	114	36	19.05	44	0	9.01
9114	54	24	6.29	32	0	8.36
9182	85	5	22.53	23	0	5.25
9201	77	30	9.94	32	0	6.91
9218	69	8	12.04	43	0	10.81
11238	**33**	**10**	**5.08**	**22**	**0**	**5.22**

a more stable behaviour of N_f in time. It is also worth of note that N_f does not show any significant correlation with the flare/CME occurrence (see again Fig. 3(b)).

As observed in Romano & Zuccarello (2011), for AR NOAA 11238 all the events occurred for low values of the difference of the number of patches with opposite signs of magnetic helicity flux (Fig. 3(c)), i.e. when the coexistence of systems characterized by opposite signs of magnetic helicity flux was more significant. No flare/CME occurred for $|N_+ - N_-| > 10$, while the flare M6.7 took place on Sept. 8 at 15:46 UT (about 87 hours from the beginning of the selected time interval) when $N_+ = N_-$. We also remark that this event, as the previous ones reported in Table 1, showed their first brightenings in the western part of the AR (see Fig. 1(b)), where the emerging positive magnetic feature was located (Fig. 1(a)) and where patches of positive and negative helicity flux were close to each other. Moreover, in the same side of the AR the northern and southern parts of the main sunspot were characterized by negative and positive magnetic helicity flux, respectively. These helicity fluxes of opposite sign in the same magnetic flux system can be ascribed to the different direction of the horizontal motions which are also responsible for a change in the sunspot shape.

We also remark that a small value of the standard deviation of $|N_+ - N_-|$ for AR NOAA 11238 in comparison with the other ARs (see Table 2) indicate that the better resolution of HMI/SDO than MDI/SOHO results in a lower noise of the $|N_+ - N_-|$ signal.

4. Conclusions

The aim of the present work is to further investigate whether that not only the flux and the accumulation of the magnetic helicity in corona are important, but also its spatial distribution. For this purpose, we applied to AR NOAA 11283 observed by HMI/SDO the same method of analysis used in Romano & Zuccarello (2011) for MDI data. The higher spatial resolution and sensitivity of HMI than MDI allowed us to clearly confirm that flares and CMEs occur when the absolute value of the difference between the number of patches of the two signs of magnetic helicity flux, $|N_+ - N_-|$, reaches the lower values. This situation reflects the coexistence of systems characterized by opposite signs of magnetic helicity flux and consequently a higher probability of interaction between them. In this regard, it is interesting to stress that some numerical simulations (Linton et al. 2001; Mok et al. 2001; Kusano et al. 2004) have shown that the interaction of magnetic fluxes with opposite helicity allows the release of the free energy because the field can relax to a state closer to a potential field through magnetic reconnection.

We also found, confirming this hypotesis, that the first brightenings of the flares observed by AIA/SDO appeared at the same location of the emergence of the positive magnetic feature near the main negative polarity where two main patches of helicity flux of opposite polarity were close to each other.

We think that the results obtained in this work clearly show that $|N_+ - N_-|$ is a good tool to study flare and CME occurrence. In fact, today all the methods used for the magnetic helicity flux computation are affected by spurious signals corresponding to fake polarities. This means that the effect of the fake polarities can be considered a sort of noise in the estimation of the fragmentation of the patches in the helicity flux maps. However, because the fake polarities usually appear in pairs of opposite sign, the absolute value of the difference between the number of patches of the two signs is independent from these spurious signals.

We plan to further investigate this topic on a wider sample of ARs by using HMI/SDO magnetograms, taking into account that in the coming years we will approach a new solar maximum and several flare/CME productive ARs will be observed.

Acknowledgements. The research leading to these results has received funding from the European Commissions Seventh Framework Programme under the grant agreement no 284461 (eHEROES project). This work was also supported by the Instituto Nazionale di Astrofisica (PRIN-INAF-2010), and by the Universitá degli Studi di Catania. F.Z. wish to thank the International Space Science Institute (Bern) for the opportunity to discuss the results on the role played bu flux emergence at the international team meeting on *Magnetic flux emergence in the solar atmosphere*.

References

Chae, J. 2001, ApJ, 560, L95
Howard, R. F., Harvey, J. W., & Forgach, S. 1990, Sol. Phys., 130, 295
Kusano, K., Maeshiro, T., Yokoyama, T., & Sakurai, T. 2004, ApJ, 610, 537
Lin, J., Soon, W., & Baliunas, S.L. 2003, New Astronomy Reviews, 47, 53
Linton, M. G., Dahlburg, R. B., & Antiochos, S. K. 2001, ApJ, 553, 905
Mok, Y., Mikic, Z., & Linker, J. 2001, ApJ, 555, 440
Nindos, A., Zhang, J., & Zhang, H. 2003, ApJ, 594, 1033
Pariat, E., Démoulin, P., & Berger, M.A. 2005, A&A, 439, 1191
Priest, E.R., & Forbes, T.G. 2000, Magnetic ReconnectionMHD Theory and Applications, Cambridge Univ. Press, Cambridge, pp. 363367
Romano, P., & Zuccarello, F. 2011, A&A, 535, 1
Schou, J., et al. 2012, Sol. Phys., 275, 229
Schuck, P.W. 2005, ApJ, 632, L53
Welsch, B. T., & Longcope, D. W. 2003, ApJ, 588, 620